Tomographic Reconstruction of Emissivity Profile from Tangentially Viewed Images using Pixel Method

Santanu BANERJEE, Asim Kumar CHATTOPADHYAY and P. VASU
Institute for Plasma Research, Bhat, Gandhinagar 382 428, Gujarat, India

(Received 18 December 2006 / Accepted 17 June 2007)

Fast camera systems for imaging tokamak plasmas are becoming increasingly popular. Edge fluctuations and plasma instabilities can be imaged in the visible and X-ray wavelengths using presently available cameras. While viewing the plasma tangentially, the lines of sight (LOS) pass through the plasma integrating the light through a number of flux surfaces. Here we report a reconstruction code for tomographic unfolding of the emissivity profile of the poloidal cross section from the tangential image, using pixel method. The poloidal cross section of the tokamak has been divided into pixels, each of which is a footprint of a subtorus. The emissivity of each of this subtorus (pixels) is assumed to be constant and uniform around the torus.

Keywords: ray-torus intersection, tomographic reconstruction, pixel method

DOI: 10.1585/pfr.2.S1120

1. Introduction

Plasma imaging is getting increasingly popular with the development of high speed cameras. Tangential viewing through the tokamak plasma cross-section provides good spatial resolution [1]. This proves to be an useful tool to study edge fluctuations and plasma instabilities in the visible and X-ray wavelengths. The reconstruction of the emissivity profile from the images is clearly a necessary task. Here an algorithm inferring the emissivity profile from the tangential images recorded on a camera chip is presented. It can easily be adapted to any machine and camera locations.

In the following, the performance of a reconstruction code implemented using MATLAB (v 7.2) is described. Section 2 briefly describes the setup of the problem. In section 3 a brief overview of the reconstruction by pixel method [2, 3] has been given. Section 4 gives a systematic analysis of the method and the obtained results. Finally, in section 5 a brief discussion is given on the results obtained on the basis of simulated data.

2. Brief Description on the Setup of the Problem

A tangential camera with a view covering a considerable portion of the poloidal cross section of the plasma is considered (refer to Fig. 1). The poloidal cross section of the tokamak torus has been divided into a matrix of 11×11 circles (hereinafter referred to as pixels; the term 'detector' being used to refer to the elements of the camera chip), each of 25 mm radius. Major radii of these sub tori (pixels) vary from 500 mm to 1000 mm in steps of 50 mm, and the z-co-ordinates of their centers range between +250 mm to −250 mm. The camera chip constitutes of a matrix of 16×16 macro pixels (cluster of pixels) of 0.48×0.48 mm dimension. The emissivity within each of these pixels is assumed to be uniform and remains constant toroidally.

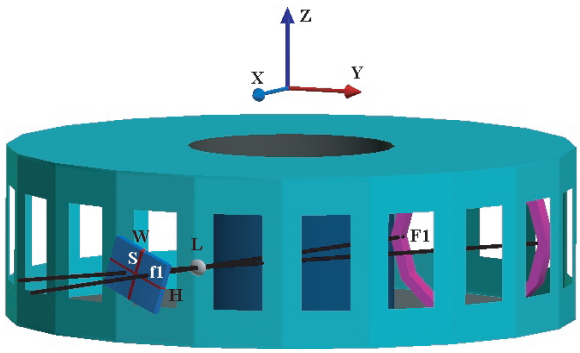

Fig. 1 Schematic of tangential view of the camera covering almost entire poloidal cross section. Three non-collinear points on the limiter (dark magenta ring) serves as the fiduciaries. $\hat{\mathbf{H}}$ and $\hat{\mathbf{W}}$ define the plane of the image formed through the lens **L. f1** is the image of **F1**, one of the fiduciaries.

Usually, in any experimental situation, the camera is setup by orienting it so that a few known points inside the tokamak vessel are imaged and these points are easily recognized in the image. Three non-collinear points, whose co-ordinates are known with respect to the machine center, serve as fiduciaries to define the camera chip and its orientation accurately to define the line of sight (LOS) of each detector through the lens center in terms of the detector unit vector **v**. Refer to appendix I for further details.

author's e-mail: sbanerje@ipr.res.in

3. Theoretical Background

3.1 Tomography problem

LOS from each detector on the camera chip passes through the optic center of the collector lens system and intercepts a number of sub tori. Calculation of brightness (f) i.e. power divided by étendue of a detector is given by

$$\sum_{j=1\sim N} I_{ij} g_j = f_i \tag{1}$$

I_{ij} is essentially the chord length of the detector i passing through the pixel number j. g_j is the emissivity of pixel j [3]. The set of simultaneous linear equations can be written as

$$\mathbf{I} * \mathbf{g} = \mathbf{f} \tag{2}$$

Where, $*$ denotes matrix multiplication. The **I** matrix is populated by solving a series of ray-torus intersection equations. A single viewing chord originating from a detector will pass through a small number of pixels toroidally on its way, thus making the **I** matrix extremely sparse.

A torus is represented by the well known equation

$$\left[R - \sqrt{(x^2 + y^2)}\right]^2 + (z - z_0)^2 = r^2 \tag{3}$$

Where, R is the major radius, z_0 is the shift along z axis and r is the minor radius. A ray in its parametric form is represented by the equation

$$\mathbf{a}_t = \mathbf{a} + t\mathbf{v} \tag{4}$$

Where, $\mathbf{a}_t$ constitutes of the components of the ray vector, **a** is the origin or eye point and **v** is the direction vector. Substituting the ray equation in the torus equation, we get a quartic equation in t. t is essentially the distance traversed by the ray from its origin along direction **v**. Then the distances between all the real roots (up to four values of t) provides the matrix element I_{ij} need to set up the matrix equation (2).

Inverting **I**, which is a sparse matrix cannot be done directly. This is an overdetermined system since, number of equations (= 256) are more than the number of unknowns (= 121). We could try in this case to minimize the chi-squared value using the equation

$$\chi^2 = (\mathbf{I} * \mathbf{g} - \mathbf{f})^T * (\mathbf{I} * \mathbf{g} - \mathbf{f}) \tag{5}$$

The superscript T denotes transposition. Solutions to the set of linear equations of this overdetermined system are found by Singular Value Decomposition (SVD) method [4, 5].

3.2 Simulation of the emissivity profile

The visible radiation from a tokamak is emitted from the edge regions with possible poloidal variations. Hence, an emissivity profile is created as

$$g(r, \theta) = 0.5 + A * e^{[-(r-r_0)^2/2\sigma^2]} * abs(\cos\theta) \tag{6}$$

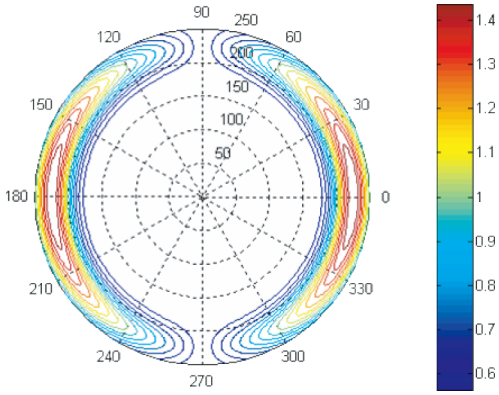

Fig. 2 Simulated edge peaked emissivity profile.

as shown in Fig. 2. Where, r is the minor radius, r_0 is the peak position of emissivity, σ defines the width of the Gaussian and θ is the angle along the poloidal cross section. It has two lobes of high emissivity region in the inboard and outboard sides with peaks at $r_0/r \sim 0.9$.

4. Results

With the simulated emissivity profile, input brightness values at the pixel centers are calculated as per equation (2). Quality of reconstruction is reflected in the *normalized residual* (*NR*), given as

$$NR = \sqrt{\sum_i \left[\left(\sum_j (I_{ij} * g_j^R) - f_i^c\right) / f_i^c\right]^2} \tag{7}$$

Where, $\mathbf{g}^R$ is the reconstructed emissivity matrix obtained through SVD [4], and $\mathbf{f}^c$ is the double precision actual brightness matrix. Output emissivity contour reconstructed at double precision brightness input (refer to Fig. 3) resembles the input emissivity with an *NR* of 4.2965×10^{-14}.

In the present scenario, two types of noises are addressed, viz. the read out like noise and the shot like noise. Several amounts of these noises are added separately to check the consistency of reconstruction. White noise with a normal distribution is added to the brightness profile. For shot like noise we have introduced a predefined percentage of the brightness value itself as the standard deviation of the Gaussian random noise

$$\mathbf{f}_{noisy} = \mathbf{f}_{clean} + \mathbf{f}_{clean} * s * randn(size(\mathbf{f}_{clean})) \tag{8}$$

For read like noise, we have introduced a predefined percentage of the mean of the overall brightness as the standard deviation of the Gaussian random noise

$$\mathbf{f}_{noisy} = \mathbf{f}_{clean} + \langle \mathbf{f}_{clean} \rangle * s * randn(size(\mathbf{f}_{clean})) \tag{9}$$

where, *randn* generates Gaussian random noise. Percentages of both the noise amount to 0.1 %, 0.3 %, 0.5 % and 1 %.

Reconstruction starts deviating from the input emissivity profile at around a noise of 0.5 percent and degrades

Table I

Normalized Residual

Read out noise		Shot noise	
Percentage	*NR*	Percentage	*NR*
1	~ 0.1475	1	~ 0.1154
0.5	~ 0.0686	0.5	~ 0.0592
0.3	~ 0.0443	0.3	~ 0.0371
0.1	~ 0.0162	0.1	~ 0.0142

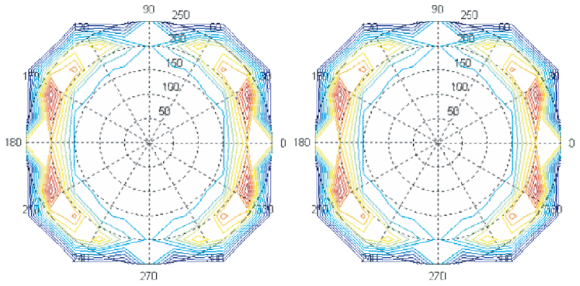

Fig. 3 Input and Output emissivity contours reconstructed at double precision brightness input.

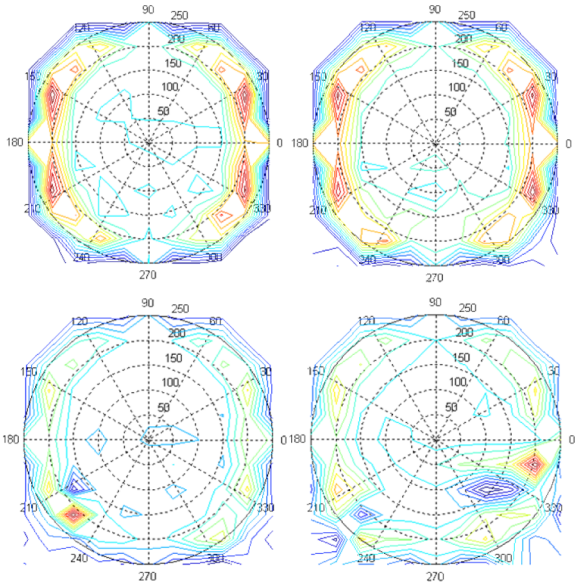

Fig. 4 Shot like noise of (L to R top row) 0.1, 0.3 % and (L to R bottom row) 0.5, 1 %.

substantially at about 1 percent in both the cases, as shown in Figs. 4 and 5. Normal residues for both the cases are tabulated in table I.

5. Discussion

Fast image acquisition at ≥ 10000 frames per second is increasingly becoming possible with the development of cameras. This allows imaging Magneto Hydro-Dynamics (MHD) activities themselves and within the exposure time for each frame of 100 μs, we can expect the main noise in the image to be shot noise and read noise. For example,

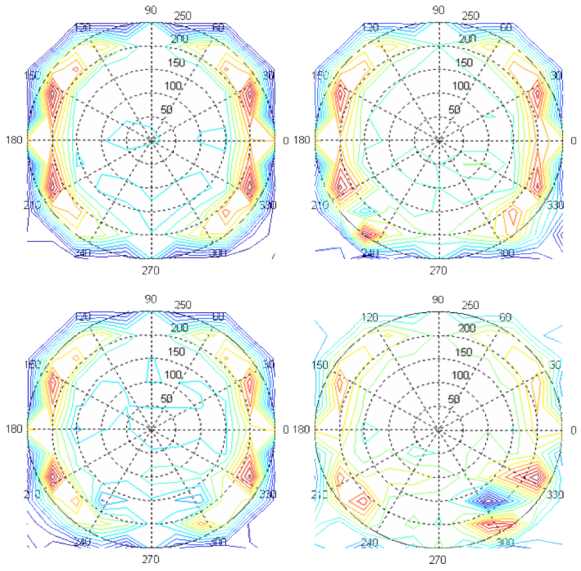

Fig. 5 Read out like noise of (L to R top row) 0.1, 0.3 % and (L to R bottom row) 0.5, 1 %.

with a chord integrated photon flux ~ 10^{14}-10^{15}photons $(cm^2)^{-1}$ s^{-1} $Sr.^{-1}$ and 0.25 mm^2 detector area on the camera chip (assuming a quantum efficiency 40-50 percent and conversion at ~ 100 electrons/count), the signal could be ~ 2×10^5-2×10^6 photoelectrons or 2,000-20,000 counts. This implies noise levels ≤ 0.3 percent of the signal. During tangential imaging, one has to take care of wall reflections, which can be small in case of carbon surfaces (low reflectivity) or can be reduced with a view dump at the far end of the LOS. This has motivated us to explore the possibility of obtaining emissivity profiles from tangentially viewed plasma images.

For an underdetermined system (number of unknown coefficients is more than the number of equations) or ill conditioned system it is difficult to get a proper solution. To solve such problems there are a number of widely used methods, for example: (i) *Linear Regularization Method* (sometime called *Phillips-Twomey method* [6], the *constrained linear inversion method* [7], *Tikhonov-Miller regularization* [8] method), (ii) *Phillips-Tikhonov Regularization Method* [9], and (iii) *Maximum Entropy Method* [3, 5 and the references therein].

We note that our system is an overdetermined system (number of unknown coefficients is less than the number of equations). For the solution of such systems *Singular Value Decomposition Method* (SVD) is the best method, though somewhat slower, because it does not fail to converge even if the matrix is ill conditioned or near singular [5].

In the present paper the quartic equation, representing the ray-torus intersection, is solved to populate the geometry matrix **I**. Run time of the code on Pentium 4 512 MB DDR2 RAM desktop computer is a few seconds only. At present the algorithm is robust to handle up to 0.5 % of noise. Both cases of read out and shot noise have been

tested. Optimization of number of pixels and detectors to handle greater amount of noise for various types of emissivity profiles is being pursued.

Acknowledgments

We gratefully acknowledge the technical and theoretical support offered by Dr. Vinay Kumar, Mr. Shrishail Padasalagi and Mr. Ketan M. Patel during the entire tenure of the work.

Appendix-I

In the following, the global origin **O** is taken as the center of the toroidal vessel. The detector locations are referred to the chip center S. Three non collinear fiduciary points F_i (X_i, Y_i, Z_i) $(i = 1,2,3)$ are identified in the vessel and they are imaged. Let their images be represented by detectors f_i on the camera chip. Center of the camera chip is denoted by the vector **OS**. Thus the vector $\mathbf{Sf}_i$ of each detector is represented in terms of the horizontal ($\hat{\mathbf{H}}$) and vertical ($\hat{\mathbf{W}}$) unit vectors of the camera chip. Unit vectors $\hat{\mathbf{H}}$ and $\hat{\mathbf{W}}$ are defined with respect to the global origin. Refer to Figure 1. Thus we have:

$$\mathbf{Sf}_i = \hat{\mathbf{H}} f_{hi} + \hat{\mathbf{W}} f_{vi} \tag{10}$$

The center of the lens of the camera is defined by the position vector **OL**. Distances Lf_i are known from the detector dimensions and the focal length of the camera lens. Thus the vectors $\mathbf{Lf}_i$ are also known from the unit vectors ($\mathbf{F}_i\mathbf{L}/|\mathbf{F}_i\mathbf{L}|$) along these directions. Thus we have:

$$\mathbf{LS} = \mathbf{Lf}_i - \mathbf{Sf}_i \tag{11}$$

Using the above, we get the horizontal and vertical unit vectors in terms of the known co-ordinates of L and the location of the images f_i on the detector of the three points F_i, given as:

$$\hat{\mathbf{H}} = \frac{(f_{v1} - f_{v3})(\mathbf{Lf}_1 - \mathbf{Lf}_2) - (f_{v1} - f_{v2})(\mathbf{Lf}_1 - \mathbf{Lf}_3)}{(f_{h1} - f_{h2})(f_{v1} - f_{v3}) - (f_{h1} - f_{h3})(f_{v1} - f_{v2})}$$

$$\hat{\mathbf{W}} = \frac{(f_{h1} - f_{h3})(\mathbf{Lf}_1 - \mathbf{Lf}_2) - (f_{h1} - f_{h2})(\mathbf{Lf}_1 - \mathbf{Lf}_3)}{(f_{h1} - f_{h3})(f_{v1} - f_{v2}) - (f_{h1} - f_{h2})(f_{v1} - f_{v3})} \tag{12}$$

Knowing $\hat{\mathbf{H}}$ and $\hat{\mathbf{W}}$ we can calculate the $\mathbf{Sd}_i$ vector for any arbitrary detector d_i and thereby **LS**. Position vector of the camera chip center is given by:

$$\mathbf{OS} = \mathbf{LS} + \mathbf{OL} \tag{13}$$

Now, position vector of each pixel with respect to the vessel center can be calculated as:

$$\mathbf{Od}_i = \mathbf{OS} + \mathbf{Sd}_i \tag{14}$$

LOS of each detector can now be represented by a ray vector with the global co-ordinates of the pixel as the eye point **a** and the unit vector along $\mathbf{d}_i\mathbf{L}$ as the direction vector **v** of equation (4).

[1] S. Ohdachi and K. Toi *et al.*, Rev. Sci, Instrum. **74**, 2136 (2003).
[2] R.S. Granetz and P. Smeulders, Nucl. Fusion **28**, 457 (1988).
[3] A.K. Chattopadhyay, A. Anand, and C.V.S. Rao, Rev. Sci. Instrum. **76**, 063502 (2005).
[4] M. Anton and H. Weison *et al.*, Plasma Phys. Control. Fusion **38**, 1849 (1996).
[5] W.H. Press, S.A. Teukolsky, W.T. Vellerling and B.P. Flannery, *Numerical Recepies in Fortran, 2nd Ed.* (Cambridge University Press, 1992).
[6] S. Twomey, Journal of the Association for Computing Machinery **10**, 97 (1963).
[7] S. Twomey, *Introduction to the Mathematics of Inversion in Remote Sensing and Indirect Measurement* (Amsterdam, Elsevier, 1977).
[8] A.W. Tikhonov and V.Y. Arsenin, *Solutions of ill-posed problems* (New York, Wiley, 1977).
[9] N. Iwama, H. Yoshida, H. Takimoto, Y. Shen, S. Takumura, and T. Tsukishima, Appl. Phys. Lett. **54**, 502 (1989).